

**ARTICLE**

# Intronic branchpoint-to-acceptor variants underlying inborn errors of immunity

Najiba Alioua<sup>1</sup> , Nathalie Lambert<sup>1</sup> , Mathilde Puel<sup>1</sup> , Sylvain Hanein<sup>2</sup> , Paul Bastard<sup>3,4,5,6</sup> , Mathieu Fusaro<sup>7,8</sup> , Marie Jaffray<sup>9</sup> , Bernardita Medel<sup>10</sup> , Lydia Khella<sup>1</sup> , Yoann Seeleuthner<sup>4,5</sup> , Mélodie Perin<sup>2</sup> , Corinne Jacques<sup>1</sup> , Marlène Pasquet<sup>11</sup> , Laura Olivier<sup>11</sup> , Fernando Sepulveda<sup>8</sup> , Tom Le Voyer<sup>4,5,6,12</sup> , Aurélie Cobat<sup>4,5,6</sup> , Patrick Nitschke<sup>2</sup> , Lionel Galicier<sup>13</sup> , Nicolas Schleinitz<sup>13</sup> , Eric Oksenfelder<sup>12</sup> , Marion Malphettes<sup>12</sup> , Bénédicte Neven<sup>3,4</sup> , Despina Moshous<sup>3,4</sup> , Felipe Suarez<sup>4,14</sup> , Claire Fieschi<sup>12</sup> , Jean-Laurent Casanova<sup>4,5,6,15,16</sup> , Geneviève de Saint Basile<sup>1,10</sup> , Guillaume Dorval<sup>17,18</sup> , Capucine Picard<sup>1,3,4,19,20\*</sup> , Jacinta Bustamante<sup>1,4,5,6\*</sup> , Peng Zhang<sup>4,5,6</sup> , and Jérémie Rosain<sup>1,4,5,6</sup> 

**Clinical laboratories searching for pathogenic variants focus mostly on the protein-coding region and corresponding essential splicing sites. Screening for variants in intronic regions requires dedicated bioinformatics tools and detailed experimental studies to confirm deleteriousness and pathogenicity. We report intronic variants in a cohort of eight patients from seven kindreds with unexplained inborn errors of immunity (IEI). Using ad hoc bioinformatics tools, we identified seven kindreds carrying three branchpoint variants at three loci (*BTK*, *SH2D1A*, and *WAS*) and four AG-gain acceptor site variants at another four loci (*DOCK8*, *NFKB1*, *STXBP2*, and *UNC13D*). The variants were located between positions -9 and -49 relative to the wild-type acceptor site. The deleteriousness and, thus, pathogenicity of these variants were confirmed by exon-captured transcriptome studies and flow cytometry analyses of protein production or function. Our findings indicate that intronic variants should be systematically screened and investigated, even in clinical laboratory settings.**

## Introduction

Genomic medicine is becoming more widely available worldwide, including for patients with suspected inborn errors of immunity (IEI) (1, 2, 3, 4, 5, 6, 7, 8, 9, 10, 11, 12, 13). Genetic diagnosis is essential for IEI to end the diagnostic odyssey and make it possible to initiate targeted and non-targeted therapies or prophylaxis and genetic counseling. However, it has been estimated that no more than 40% of patients with suspected IEI receive a genetic diagnosis (9). Clinical laboratories focus their search for germline pathogenic variants on single-nucleotide variants (SNV), indels, and structural variants affecting the coding sequence (CDS) and essential splicing sites (1). The identification of variants in intronic regions could increase

diagnosis rates for patients with IEI (14, 15, 16). Such variants can have pathogenic effects via various biological mechanisms. In particular, variants may disrupt intronic branchpoints (BPs) (17) or lead to the gain of AG acceptor nucleotides between BP and canonical splice acceptor sites (18). Intronic BP-to-acceptor variants are the most proximal, as 88% of BP variants are located between positions -40 and -15 relative to the canonical acceptor site (17). Such variants can, therefore, be covered even by high-throughput sequencing (HTS) approaches capturing exons, such as panel or whole-exome sequencing. However, screening for such intronic variants requires dedicated bioinformatics tools, and several such tools have recently been developed (17, 18,

<sup>1</sup>Study Center for Primary Immunodeficiencies, Necker Hospital for Sick Children, Assistance Publique Hôpitaux de Paris, Paris, France; <sup>2</sup>Bioinformatic Platform, Institute of Genetic Diseases, Inserm U1163, Imagine, University of Paris Cité and Necker Federative Research Structure, Paris, France; <sup>3</sup>Pediatric Immunology-Hematology and Rheumatology Unit, Necker Hospital for Sick Children, Assistance Publique Hôpitaux de Paris, Paris, France; <sup>4</sup>Imagine Institute, Inserm U1163, University of Paris Cité, Paris, France; <sup>5</sup>Laboratory of Human Genetics of Infectious Diseases, Necker Branch, Inserm U1163, Necker Hospital for Sick Children, Paris, France; <sup>6</sup>St. Giles Laboratory of Human Genetics of Infectious Diseases, Rockefeller Branch, Rockefeller University, New York, NY, USA; <sup>7</sup>Immunology Department Laboratory, Referral Medical Biology Laboratory, Institut Fédératif de Biologie, Toulouse University Hospital Center, Toulouse, France; <sup>8</sup>INFINITY, Toulouse Institute for Infectious and Inflammatory Diseases, Inserm U1291, CNRS U5051, University Toulouse III, Toulouse, France; <sup>9</sup>Department of Pediatrics, Dieppe Hospital, Dieppe, France; <sup>10</sup>Laboratory of Molecular Basis of Altered Immune Homeostasis, Imagine Institute, Inserm U1163, University of Paris Cité, Paris, France; <sup>11</sup>Department of Pediatric Hematology and Immunology, Children's Hospital, University Hospital, Toulouse, France; <sup>12</sup>Immunopathology Department, Saint-Louis Hospital, Assistance Publique Hôpitaux de Paris, University of Paris Cité, Paris, France; <sup>13</sup>Department of Internal Medicine and Immunology, Timone Hospital, Assistance Publique des Hôpitaux de Marseille, Marseille Immunopole, Marseille, France; <sup>14</sup>Department of Clinical Hematology, Necker Hospital for Sick Children, Assistance Publique Hôpitaux de Paris, Paris, France; <sup>15</sup>Department of Pediatrics, Necker Hospital for Sick Children, Assistance Publique Hôpitaux de Paris, Paris, France; <sup>16</sup>Howard Hughes Medical Institute, New York, NY, USA; <sup>17</sup>Laboratory of Hereditary Kidney Diseases, Imagine Institute, Inserm U1163, University of Paris Cité, Paris, France; <sup>18</sup>Laboratory of Genomic Medicine for Rare Diseases, Necker Hospital for Sick Children, Assistance Publique Hôpitaux de Paris, Paris, France; <sup>19</sup>Laboratory of Lymphocyte Activation and Susceptibility to EBV Infection, Inserm U1163, Imagine Institute, Paris, France; <sup>20</sup>Centre de Références des Déficits Immunitaires Héréditaires, Necker Hospital for Sick Children, Assistance Publique Hôpitaux de Paris, Paris, France.

\*C. Picard and J. Bustamante contributed equally to this paper. Correspondence to Jérémie Rosain: [jeremie.rosain@institutimagine.org](mailto:jeremie.rosain@institutimagine.org).

© 2025 Alioua et al. This article is available under a Creative Commons License (Attribution 4.0 International, as described at <https://creativecommons.org/licenses/by/4.0/>).

19, 20). Additional wet-laboratory studies are also required to confirm the pathogenicity of the variants identified (14, 21), which can be challenging in clinical laboratory settings.

## Results

### Seven unrelated kindreds with IEI

We retrospectively report eight patients in whom we have ultimately identified BP and AG-gain variants in genes of IEI. The patients were initially referred to a clinical laboratory (Study Center for Primary Immunodeficiencies, Paris, France) based on their clinical phenotype and laboratory test results during basic immunological investigations. The eight patients (P1-P8) were from seven unrelated kindreds (A-G). The case reports are described in detail in Table S1 and the supplementary material. All the patients were living in France. The patients had a mean age of 29 years (range: 8–58 years); seven patients were male and one was female. One patient (P5) was born to consanguineous parents. P1 from kindred A had a history of invasive bacterial disease and agammaglobulinemia. P2 from kindred B had a history of Epstein-Barr virus-negative diffuse large B cell lymphoma (DLBCL) and hypogammaglobulinemia. P3 from kindred C had eczema and thrombocytopenia. P4 from kindred D had a history of bronchiectasis, cutaneous and genital human papillomavirus (HPV) infections, and combined immunodeficiency. P5 and P6 from kindreds E and F, respectively, had a history of hemophagocytic lymphohistiocytosis (HLH). P7 and his father, P8, from kindred G had a history of common variable immunodeficiency (CVID). All patients were screened for IEI by targeted HTS encompassing all genes for which IEI are known (22). However, an analysis of SNV, indels, and copy-number variants (CNVs) within CDSs and essential splice sites identified no candidate pathogenic variants. Due to their clinical and immunological phenotypes, these patients were subsequently and sporadically referred back to our laboratory.

### Identification of BP or AG-gain variants in the seven kindreds

Targeted HTS involves the capturing of exons with a mean coverage >400X, resulting in partial coverage of the flanking intronic regions (10). We therefore reanalyzed HTS data of the patients, searching for candidate intronic variants, given the high level of suspicion for IEI in all kindreds. Variants were primarily screened using AGAIN (18), BPHunter (17), SpliceAI (19), and Pangolin (20) and were also subsequently analyzed with CADD v1.7 (23), phastCons (24), and phyloP (25). Interestingly, we identified candidate intronic variants in all kindreds: BP candidate variants at three loci (*BTK*, *SH2D1A*, and *WAS*) in kindreds A, B, and C, respectively, and AG-gain candidate variants at another four loci (*DOCK8*, *STXBP2*, *UNC13D*, and *NFKB1*), in kindreds D, E, F, and G, respectively (Table 1 and Fig. 1). One variant was present in the homozygous state (*STXBP2*), three were hemizygous (*BTK*, *SH2D1A*, and *WAS*), two were heterozygous in trans with another heterozygous variant located in the CDS (a large deletion in *DOCK8* and a missense variant in *UNC13D*), and one was present in the heterozygous state (*NFKB1*) (Table 1 and Fig. 1). In P4, a revertant in *DOCK8* c.2971-6C>G

Table 1. Summary of the features of the intronic variants identified with the various associated scores

Kindred	Type of variant	Locus	Zygosity	gDNA position (hg38)	cDNA (MANE)	BPHunter score	AGAIN score	Absolute SpliceAI max/ Pangolin max	CADD v1.7	phyloP	phastCons	MAF gnomAD v4.1.0
A	BP	<i>BTK</i>	Hemizygous	chrX-101354717- G	c.1567-24del 4	4	NA	0.43/0.47	14.78	1.63	1	0
B	BP	<i>SH2D1A</i>	Hemizygous	chrX-124365739-A- G	c.138-22A>G	4	NA	0.81/0.64	20.2	5.24	1	0
C	BP	<i>WAS</i>	Hemizygous	chrX-46685714-T-G	c.361-20T>G	7	NA	0.54/0.36	7.994	3.08	0.99	0
D	AG-gain	<i>DOCK8<sup>a</sup></i>	Heterozygous	chr9-396780-C-A	c.2971-5C>A	NA	5	0.99/0.83	20.83	1.77	0.03	0
E	AG-gain	<i>STXBP2</i>	Homozygous	chr19-7644605-T-A	c.1108-9T>A	NA	4	0.50/0.64	5.750	-0.61	0	0
F	AG-gain	<i>UNC13D<sup>b</sup></i>	Heterozygous	chr17-75331397-G-T	c.2448-49C>A	NA	4	1/0.85	8.359	-0.28	0	0
G	AG-gain	<i>NFKB1</i>	Heterozygous	chr4-102578848-T- A	c.572-33T>A	NA	3	0.99/0.85	4.551	1.44	0.44	0

MANE, Matched Annotation from NCBI; EMBL-EBI; MAF, minor allele frequency  
<sup>a</sup>In trans with a heterozygous deletion encompassing exons 13–43.  
<sup>b</sup>In trans with the c.2971A>C p.H976P variant.

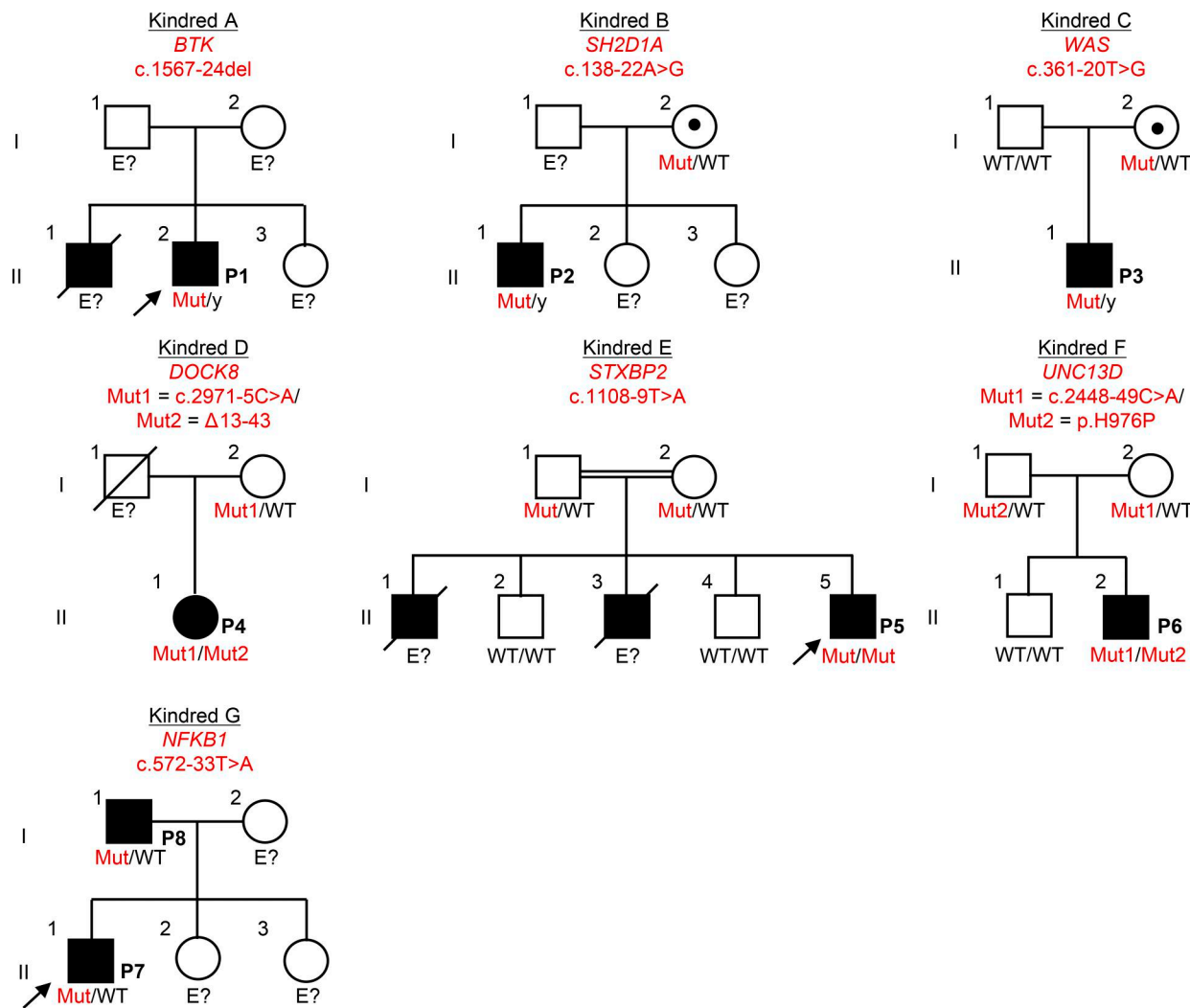


**Figure 1. Pedigree of seven French kindreds with IEI.** Male and female individuals are represented by squares and circles, respectively. Each generation is designated by a Roman numeral and each individual by an Arabic numeral. Individuals with immune dysregulation are shown as closed black symbols, and the index case is indicated by an arrow. Individuals whose genetic status could not be tested are designated "E?". Mut = mutated.

was also evidenced on genomic DNA extracted from T cell blasts (T-blasts). This revertant was flanking the germline intronic variant (c.2971-5C>A) (Fig. S1). All the germline intronic BP-to-acceptor variants were predicted to be deleterious by BPHunter (for BP variants) and AGAIN (for AG-gain variants), and all had SpliceAI and Pangolin scores above the cutoff of  $|0.2|$  (range = 0.36–0.99) (Table 1). BP variants were scored higher than AG-gain variants by CADD, phyloP, and phastCons (Table 1). All the variants identified were rare and were absent from the Genome Aggregation Database (gnomAD) v4.1 (26), BRAVO/TOPmed freeze 8 (27), UK Biobank (28), or All of Us (29) databases. None of these variants were reported in HGMD professional v2024.4 (30). Providing further support for their pathogenicity, these variants segregated with the clinical phenotype in the various kindreds (Fig. 1). We, thus, identified rare and previously unknown candidate intronic variants in IEI genes with recessive or dominant inheritance in all the kindreds studied.

#### Investigating the candidate intronic variants at the mRNA and protein levels

We then studied the consequences of these variants for RNA splicing, protein production, and/or function. We used peripheral blood cells from the patients or their siblings or cells derived from blood cells. For RNA splicing, we used the exon-captured transcriptome of the peripheral blood mononuclear cells (PBMCs) or T-blasts from the patients or their siblings. We performed transcriptomic analyses in all kindreds except kindred A. Exon 2 skipping occurred in the T-blasts of P2, who was hemizygous for the BP variant c.138-22A>G of *SH2D1A* (Fig. 2 A). In T-blasts from P3, who was hemizygous for the BP variant c.361-20T>G of *WAS*, we observed a retention of intron 3 that was predicted to cause a frameshift (Fig. 2 B). In the T-blasts of P4, exons 13–43 were skipped in the *DOCK8* transcript due to the large deletion (Fig. S2), and there was a predicted frameshift insertion of 4 bp (r.2970\_2971insACAG, p.V991Gfs\*11), probably due to the c.2971-5C>A variant (Fig. 2 C). There was also normal remaining skipping of exon 24–25 (Fig. 2 C), likely due to the

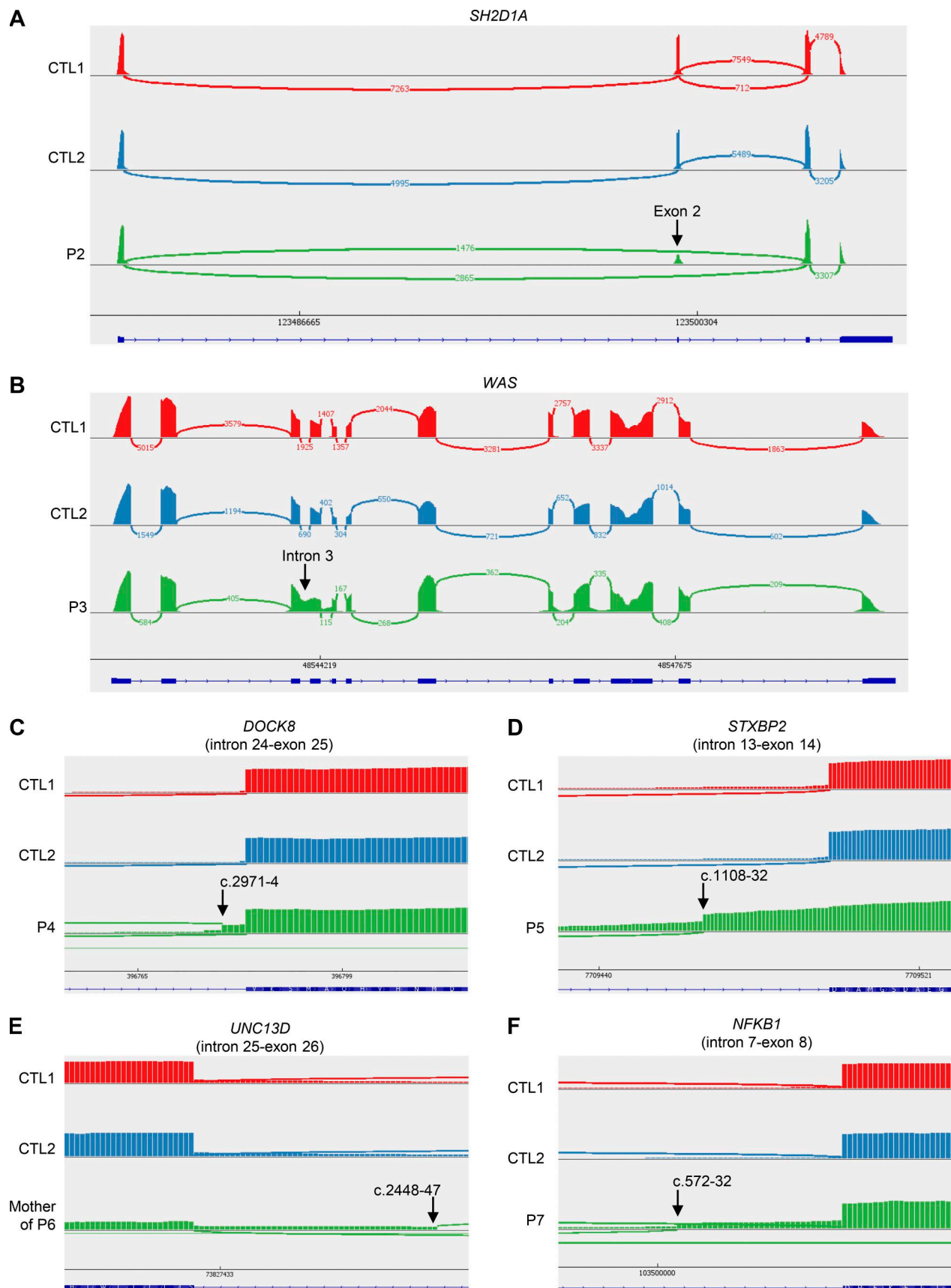


**Figure 2. Sashimi view of RNA sequencing in six different kindreds with intronic variants affecting BP sites or AG-gain variants located between the BP and the acceptor splice site. (A-F)** RNA-sequencing data from (A) T-blasts of P2 and two controls (CTL), (B) T-blasts of P3 and two controls (CTL), (C) T-blasts of P4 and two controls (CTLs), (D) T-blasts of P5 and two controls (CTLs), (E) PBMCs of the mother of P6 and two controls (CTLs), and (F) T-blasts of P7 and two controls (CTLs).

Alioua et al.

Intronic branchpoint-to-acceptor variants

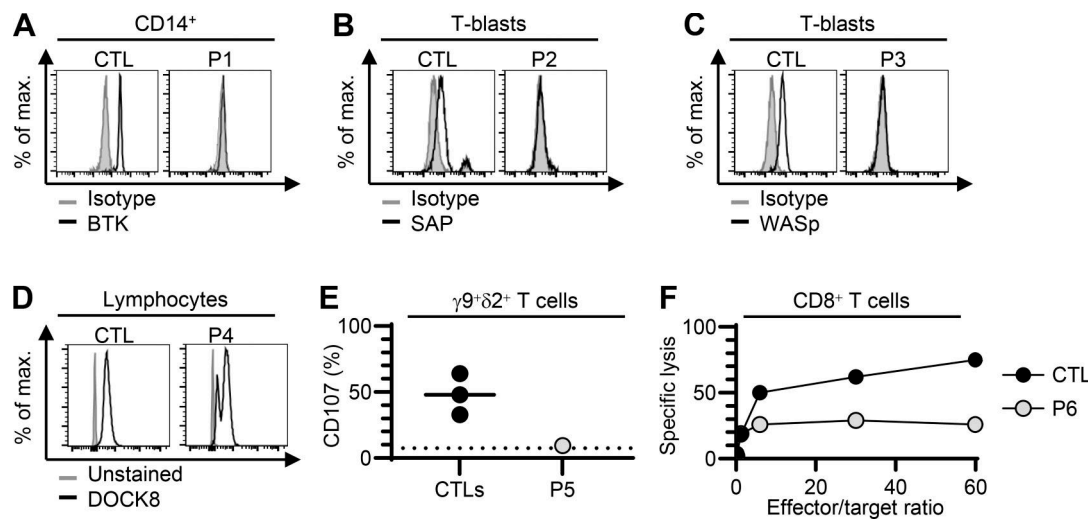


**Figure 3. Intracellular protein expression or functional assays for the index cases from kindreds.** **(A–F)** Flow cytometry study of (A) BTK gated on CD14<sup>+</sup> monocytes from fresh whole blood from P1 and a control (CTL), (B) SAP in T-blasts from P2 and a CTL, (C) WASp in T-blasts from P3 and a CTL, and (D) DOCK8 in lymphocytes from the fresh whole-blood cells of P4. **(E)** Degranulation assay on V $\gamma$ 9<sup>+</sup>V $\delta$ 2<sup>+</sup> T cells stimulated with 1-Hydroxy-2-methyl-2-but enyl 4-pyrophosphate lithium salt (HMBPP) in three CTLs and P5. **(F)** <sup>51</sup>Cr-based cytotoxic activity of Fas-deficient L1210-3 target cells in CD8<sup>+</sup> T cells from a CTL or P6. The results are expressed as the percent-specific lysis. The effector/target ratio is shown on the x axis and was calculated from the number of CD8<sup>+</sup> T cells, as determined by flow cytometry.

revertant. In the T-blasts of P5, who was homozygous for the AG-gain variant c.1108-9T>A of *STXBP2*, a new acceptor splice site was created at c.1108-32, leading to a 32-nt frameshift insertion (r.1107\_1108ins32, p.D370Rfs\*6) (Fig. 2 D). In PBMCs from the mother of P6, who was heterozygous for the c.2448-49C>A variant of *UNC13D*, we observed the creation of a new acceptor splice site at c.2448-47, leading to a 47-nucleotide insertion with a frameshift (r.2447\_2448ins47, p.L817Hfs\*18) (Fig. 2 E). In the T-blasts of P7, who is heterozygous for the AG-gain variant c.572-33T>A of *NFKB1*, a new acceptor splice site was created at c.572-32, leading to a 32-nucleotide insertion with a frameshift (r.571\_572ins32, p.D191Efs\*3) (Fig. 2 F), and exon 8 was skipped, also leading to a frameshift (Fig. S2 B). Furthermore, we observed impaired production of the following proteins: (1) BTK in CD14<sup>+</sup> monocytes from P1 (Fig. 3 A), (2) SAP in T-blasts from P2 (Fig. 3 B), (3) WASp in T-blasts from P3 (Fig. 3 C), and (4) DOCK8 in lymphocytes from P4 (Fig. 3 D). P4 had two peaks of DOCK8 protein levels of different intensities, confirming at protein level the reversion (31). In addition, degranulation and cytotoxic assays revealed an impairment of V $\gamma$ 9<sup>+</sup>V $\delta$ 2<sup>+</sup> T cells from P5 and CD8<sup>+</sup> T cells from P6, respectively (Fig. 3, E and F). We therefore found evidence of either impaired RNA splicing (kindreds B, C, D, E, F, and G) or impaired protein production (kindreds A, B, C, and D) or function (kindreds E and F) in all the kindreds tested. These data support the hypothesis that the intronic variants identified are pathogenic or likely pathogenic, in accordance with American College of Medical Genetics and Genomics (ACMG) criteria (14, 21).

#### Comparison of predicted and observed impacts on splicing

All BP and AG-gain variants were flagged as possibly pathogenic by several scores, including SpliceAI (19) and Pangolin (20), both of which provide an indication of the likely impact on the RNA.

We, thus, compared the in silico predictions of these two scores (Table S2) with the results of a wet-laboratory RNA study for these variants (Figs. 2, S1, and S2; and Table 2). The observed impact of the *SH2D1A* BP variant in T-blasts from P2 (exon 2 skipping) was correctly predicted in silico by SpliceAI and Pangolin, both of which predicted an impact on the wild-type (WT) acceptor and donor splice sites of exon 2. For the WAS BP variant c.361-20T>G, both SpliceAI and Pangolin predicted the loss of the WT acceptor site of exon 4 but no impact on the donor site, consistent with the observed retention of intron 3 in the cells of P3. For the AG-gain variant c.2971-5C>A in *DOCK8*, both SpliceAI and Pangolin predicted the use of an alternative AG with an in-frame insertion of three nucleotides, but a four-nucleotide insertion was actually observed in the T-blasts of P4. Interestingly, the intronic *DOCK8* revertant (c.2971-6C>G) was predicted by SpliceAI to annihilate the AG-gain effect of the c.2971-5C>A. For the AG-gain variant of *STXBP2*, both SpliceAI and Pangolin predicted a major weakening of the WT acceptor site. However, discordant predictions were obtained for alternative AG sites. Indeed, SpliceAI predicted the creation of a new acceptor splice site at position c.1108-7, whereas Pangolin predicted the creation of a new acceptor splice site at position c.1108-32 (Fig. S3), which is what was actually observed in the T-blasts of P6. For the AG-gain variant of *UNC13D*, both SpliceAI and Pangolin predicted a weakening of the WT acceptor site and the creation of an acceptor site at c.2448-47, which was confirmed by the RNA study on T-blasts from P7. For the AG-gain variant of *NFKB1*, both SpliceAI and Pangolin predicted the creation of an acceptor splice site at c.572-31, whereas an acceptor splice site was actually created at c.572-32 in the T blasts of P7. Overall, the impact on RNA levels was correctly predicted for three of the six germline variants by SpliceAI and four of the six variants by Pangolin.

Table 2. Summary of the consequences of the various intronic variants detected at RNA level

Kindred	Cells and individuals studied	Gene and transcript references	Variant investigated	Consequences at RNA level
B	T-blasts from P2	SH2D1A (NM_002351.5)	c.138-22A>G	Skipping of exon 2, frameshift predicted
C	T-blasts from P3	WAS (NM_000377.3)	c.361-20T>G	Retention of intron 3, frameshift predicted
D	T-blasts from P4	DOCK8 (NM_001290223.2)	c.2971-5C>A Δ13-43	Creation of a new acceptor splice site at -4, frameshift predicted (r.2970_2971insACAG, p.V991Gfs*11)
E	T-blasts from P5	STXBP2 (NM_006949.4)	c.1108-9T>A	Creation of a new acceptor splice site at c.1108-32, frameshift predicted (r.1107_1108ins32, p.D370Rfs*6)
F	PBMCs from the mother of P6	UNC13D (NM_199242.3)	c.2448-49C>A	Creation of a new acceptor splice site at c.2448-47, frameshift predicted (r.2447_2448ins47, p.L817Hfs*18)
G	T-blasts from P7	NFKB1 (NM_003998.4)	c.572-33T>A	Creation of a new acceptor splice site at c.572-32, frameshift predicted (r.571_572ins32, p.D191Efs*17) Skipping of exon 8, frameshift predicted

## Discussion

We describe here seven new pathogenic or likely pathogenic intronic variants either disrupting BP or leading to an AG-gain between the BP and the canonical acceptor site. The identification of these variants provided the various kindreds included in this study with a genetic diagnosis. BPHunter (17), AGAIN (18), SpliceAI (19), and Pangolin (20) were powerful tools after filtering based on the MAF of the variants. Nucleotide conservation-derived scores, such as phastCons (24) and CADD (23, 32), can also be helpful, providing high scores for BP variants, but no interpretation of the likely effects of BP variants. There should be more systematic screening and investigation of intronic variants. Indeed, such variants can be called even with lower coverage study, as suggested *in silico* by a 30X down-sampling analysis (Table S3). The major advantage of IEI over other genetic diseases is that most IEI-related genes are expressed in peripheral blood cells and can be investigated through RNA studies and protein expression analysis. For genes that are poorly expressed in peripheral blood cells, or for variants that are subject to RNA nonsense-mediated decay, treatment with an RNA inhibitor, such as emetine, can help to increase the number of reads (33). In clinical laboratory settings, such RNA studies are essential to confirm that the variant is pathogenic (PVS1 ACMG/AMP criterion) (14, 15). They can also facilitate the investigation of variants at loci homologous to one or several pseudogenes (34, 35, 36) or screening for random monoallelic expression (37). The demonstration of an impairment of protein production or function by clinical flow cytometry also provides additional evidence of pathogenicity (38, 39). A blind, hypothesis-free approach to RNA sequencing would also be worthwhile but challenging, as it requires many in-house controls and a dedicated bioinformatics pipeline, although such approaches have been shown to increase diagnostic yield slightly (40). In addition to the problem of possible variants of genes that are not expressed, such RNA studies are limited by the cell type specificity of splicing (35). Our findings demonstrate the importance of the systematic screening and investigation of intronic variants in clinical laboratory settings for patients with suspected IEI but no genetic diagnosis.

## Materials and methods

### Case reports

#### Kindred A

We investigated a 54-year-old patient (P1) with non-consanguineous Welsh parents living in France. His sister had undergone allogeneic bone marrow transplantation for leukemia and is now being treated for colon cancer. The older brother of P1 was diagnosed with agammaglobulinemia on the basis of immunological tests during infancy. He was given lifelong intravenous immunoglobulin treatment, which led to the transmission of hepatitis C virus, leading to cirrhosis and, ultimately, to the death of this individual. P1 has a history of chronic lung infections, including bronchial superinfections treated by antibiotics. Pulmonary function tests were normal. Given the clinical context and family history, immunological assessments were performed and showed: (1) hypogammaglobulinemia (IgG < 0.26 g/liter [normal range, NR: 7-16 g/liter], IgA < 0.05 g/liter [NR: 0.7-4 g/liter], and IgM < 0.06 g/liter [NR: 0.4-2.3 g/liter]), (2) severe B cell lymphopenia (CD19<sup>+</sup> = 0/mm<sup>3</sup>; NR: 169-271/mm<sup>3</sup>) with normal T and natural killer (NK) cell counts, and (3) an absence of antibody production (data not shown). P1 received immunoglobulin supplementation, initially intravenously and then subcutaneously. After 15 years of treatment, his IgG levels are normal on supplementation, and he remains free of pulmonary infections. Over the last 2 years, P1 has been complaining of undocumented chronic diarrhea not relieved by medication. Plans to provide IgA and IgM supplementation are currently being implemented.

#### Kindred B

We investigated a single patient (P2) born in 2006 to non-consanguineous European parents living in France. The parents of the proband and his two sisters were healthy and had no remarkable medical history. P2 had a history of recurrent ear, nose, and throat (ENT) infections during infancy, including several acute middle ear infections treated by antibiotics that led to tympanoplasty. He also had two episodes of undocumented bronchitis and two episodes of scarlet fever. At the age of 16 years, he reported pain in the right tibia of several months'

duration, with no general signs apart from asthenia and weight loss. A magnetic resonance imaging scan of the knee was performed, revealing a subperiosteal collection beneath the anterior tibial periosteum, with irregular intraosseous extension. A bone biopsy was performed, and pathology examinations led to the diagnosis of a DLBCL of the germinal center subgroup. Immunological tests were performed. Blood cell counts and immunoglobulin levels were normal (IgG 7.3 g/liter [NR: 7.0–16.0 g/liter], IgA 0.82 g/liter [NR: 0.8–3.0 g/liter], and IgM 1.99 g/liter [NR: 0.5–2 g/liter]) (Table S2), but isolated hypogammaglobulinemia due to IgG4 deficiency (IgG1 4.74 g/liter [NR: 4.9–11.4 g/liter], IgG2 1.3 g/liter [NR: 1.5–6.4 g/liter], IgG3 0.54 g/liter [NR: 0.2–1.2 g/liter], and IgG4 0.06 g/liter [NR: 0.08–1.0 g/liter]) was observed. Immunophenotyping showed that B and NK cell counts were normal but that the patient had severe T cell lymphopenia ( $CD3^+CD4^+$  245/mm<sup>3</sup> [NR: 500–1,500/mm<sup>3</sup>],  $CD3^+CD8^+$  312/mm<sup>3</sup> [NR: 200–800/mm<sup>3</sup>],  $CD19^+$  128/mm<sup>3</sup> [NR: 100–800/mm<sup>3</sup>], and  $CD16^+CD56^+$  224/mm<sup>3</sup> [NR: 50–400/mm<sup>3</sup>]).

#### Kindred C

P3 was born in 2015 to non-consanguineous parents. At the age of 4 mo, he developed eczema. P3 has a history of upper and lower respiratory tract infections, and one episode of undocumented arthritis presumed to be bacterial. A computed tomography scan revealed bronchiectasis. This patient has also experienced episodes of epistaxis. Immunological tests revealed microthrombocytopenia and T cell lymphopenia, with abnormally low percentages of naïve T cells. Levels of IgG, IgA, and IgM, and of toxoid tetanus, were normal. The patient is currently treated by subcutaneous immunoglobulin supplementation, oral antibiotic prophylaxis (penicillin G and cotrimoxazole), and aerosolized salbutamol and steroids.

#### Kindred D

P4 was born in 1985 to non-consanguineous parents. She has a history of several cutaneous and gynecologic HPV infections requiring frequent conizations and, more recently, urothelial cancer requiring surgery. She has also suffered from bronchiectasis with bronchial superinfections and *Pseudomonas aeruginosa* colonization. Immunophenotyping showed normal CD8<sup>+</sup> T and NK cell counts, but CD4<sup>+</sup> T and B cell lymphopenia ( $CD3^+CD4^+$  206.32/mm<sup>3</sup> [NR: 460–1,230/mm<sup>3</sup>],  $CD3^+CD8^+$  614.26/mm<sup>3</sup> [NR: 190–850/mm<sup>3</sup>],  $CD19^+$  54.23/mm<sup>3</sup> [NR: 92–420/mm<sup>3</sup>], and  $CD16^+CD56^+$  203.97/mm<sup>3</sup> [NR: 89–362/mm<sup>3</sup>]). Immunoglobulin levels were subnormal (IgG: 9.7 g/liter [NR: 5.4–13.2 g/liter], IgA 2.7 g/liter [NR: 0.5–2.2 g/liter], and IgM 0.42 g/liter [NR: 0.53–1.62 g/liter]).

#### Kindred E

P5 was born in 2006 to consanguineous Moroccan parents living in Morocco. P5 had four brothers. The eldest (I.1) died at the age of 11 years from Wilson's disease and a possible undocumented IEI. Another brother died at the age of 5 years from macrophagic activation syndrome, part of the spectrum of HLH. No genetic investigation was performed on either of these brothers. The parents of the proband and his other two brothers are healthy, and the patient had no other remarkable medical history. Since

the age of 2 years, P5 has had a history of recurrent ENT infections, including pharyngitis, sore throats, and ear infections treated with antibiotics on an outpatient basis. At the age of 4 years, splenomegaly with progressive enlargement occurred. The patient also had three episodes of undocumented left basal lung disease during a single year that were treated with intravenous antibiotics, with a good clinical outcome. P5 is now suffering from lung disease, which is probably chronic due to repeated infections. He also has splenic involvement, with an enlarged spleen, possible hepatic involvement causing portal hypertension, and anemia due to iron deficiency. Immunological testing was performed when P5 was referred to our laboratory in France. Blood cell counts revealed cytopenia, including anemia, neutropenia, and thrombocytopenia (hemoglobin 6 g/dl [NR: 11.5–15.5 g/dl], neutrophils 0.740 [NR: 2–8 T/liter], and platelets 86 T/liter [NR: 150–450 T/liter]). Immunoglobulin levels were normal (IgG 11.6 g/liter [NR: 5.4–13.2 g/liter], IgA 0.77 g/liter [NR: 0.5–2.2 g/liter], and IgM 1.15 g/liter [NR: 0.53–1.62 g/liter]) (Table S2). In addition, immunophenotyping revealed normal T and NK cell counts but severe B cell lymphopenia ( $CD3^+CD4^+$  1,183/mm<sup>3</sup> [NR: 650–1,500/mm<sup>3</sup>],  $CD3^+CD8^+$  1,332/mm<sup>3</sup> [NR: 370–1,100/mm<sup>3</sup>],  $CD19^+$  35/mm<sup>3</sup> [NR: 273–860/mm<sup>3</sup>], and  $CD16^+CD56^+$  220/mm<sup>3</sup> [NR: 100–480/mm<sup>3</sup>]).

#### Kindred F

P6 was born in 2003 to non-consanguineous parents. The parents of the proband and his brother were healthy and had no remarkable medical history. Since birth, P6 has suffered from HLH, treated by haploidentical hematopoietic stem cell transplantation with cells from his father at the age of 6 mo. This procedure was successful and P6 remains in good health to this day.

#### Kindred G

P7, born in 2004, has a history of upper respiratory tract infections since infancy. At the age of 5 years, he was hospitalized for meningitis due to enterovirus. At the age of 20 years, he displayed pneumonia with septicemia due to *Streptococcus pneumoniae*, which was successfully treated with antibiotics. Immunological testing was performed at the age of 17 years and revealed low immunoglobulin levels, normal counts of B cells, abnormally low percentages of switched memory B cells, and an excess of  $CD21^{\text{low}}$  cells. P7 was initially treated with cotrimoxazole and then with immunoglobulin supplementation from the age of 20 years onward. P7's father, P8, born in 1966, also had a history of CVID with low levels of immunoglobulin.

#### Patient recruitment

Patients were recruited through a clinical laboratory, which is the reference laboratory in France for the investigation of IEI. All patients or their guardians provided written informed consent. The investigations described here were performed in France, in accordance with local regulations.

#### HTS on genomic DNA

HTS was performed for a panel encompassing all known IEI genes, as previously described (10). The different version of the

panel encompasses from 300 to 500 genes. DNA was extracted from EDTA-treated peripheral blood samples, either manually via the phenol-chloroform method or with a Chemagic Prime instrument (Perkin Elmer). Genomic DNA libraries were generated from 2 µg DNA sheared with a Covaris S2 Ultrasonicator, with the SureSelectXT HS2 Library PrepKit (Agilent), on the Genomic Platform at the Imagine Institute, Paris. Capture was performed by hybridization, with 120-bp biotinylated complementary RNA baits designed with SureSelect SureDesign software (Agilent, *Homo sapiens*, hg19, GRCh37, February 2009) to cover all exons and splicing junctions of the genes implicated in IEIs. The targeted regions of interest were pulled out with magnetic streptavidin beads, amplified by PCR with indexing primers, and sequenced on an Illumina HiSeq2500 HT system (paired-end sequencing, 2 × 130 bases).

Data were analyzed at the University of Paris Cité/Imagine Institute Bioinformatics core facilities. Paired-end sequences were mapped onto the human reference genome (NCBI build37/hg19 version) with the Burrows-Wheeler aligner. Downstream processing was performed with the Genome Analysis Toolkit (GATK), SAMtools (41), and Picard tools, according to documented best practice (<https://software.broadinstitute.org/gatk/best-practices/>). Variant calls were made with the GATK UnifiedGenotyper, based on the 72nd version of the ENSEMBL database. Genome variants were defined with our in-house PolyDiag software for NGS, which filters out irrelevant and common polymorphisms on the basis of frequencies in public databases: the US National Center for Biotechnology Information Database of Single-Nucleotide Polymorphisms (42), 1000 Genomes (43), and the gnomAD (<https://gnomad.broadinstitute.org/>) (44, Preprint).

We evaluated CNVs (i.e., large duplications or deletions) for each individual by determining the relative read count for each targeted region as the ratio of the read count for that region divided by the total absolute number of read counts for all the targeted regions. The ratio of the relative read count for a region in a given individual to the mean relative read count in other individuals from the same run gave the estimated CNV for the region concerned in the individual considered (method adapted from [45]). Homozygous deletion was suspected when this ratio was close to zero (no aligned reads). For the detection of monoallelic CNVs, a ratio below 0.7 was considered suggestive of heterozygous deletion, whereas a ratio above 1.3 was considered suggestive of heterozygous duplication.

#### In silico screening of pathogenic variants

Variants were aligned with the hg37 or hg38 reference sequence, and the following scores were determined: AGAIN (<https://hgidsoft.rockefeller.edu/AGAIN/>; <https://github.com/casanova-lab/AGAIN>) (18), BPHunter (<https://hgidsoft.rockefeller.edu/BPHunter/>; <https://github.com/casanova-lab/BPHunter>) (17), SpliceAI (<https://spliceailookup.broadinstitute.org/>; <https://github.com/Illumina/SpliceAI>) (19); and Pangolin (<https://spliceailookup.broadinstitute.org/>; <https://github.com/tkzeng/Pangolin>), CADD v1.7 (<https://cadd.gs.washington.edu/>) (23), phastCons (<https://compgen.cshl.edu/phast/>) (24), and phyloP (<https://compgen.cshl.edu/phast/>) (25).

Possible pathogenic intronic variants were primarily screened using SpliceAI, Pangolin, AGAIN, and BPHunter. Regarding the cutoffs used, for SpliceAI (and by homology for Pangolin), any absolute score >0.2 was considered as significantly elevated. This latter score is the permissive recommended cutoff by ACMG (14, 15). For AGAIN and BPHunter, any score >3 was considered as significantly elevated. Results for other scores (CADD v1.7, phastCons, and phyloP) are also provided for descriptive purposes but were not specifically used to screen for variants.

#### Cell culture

PBMCs were isolated with Ficoll (#CMSMSL01-OU; Eurobio). T-blasts were generated from fresh or cryopreserved PBMCs with ImmunoCult-XF T-Cell Expansion Medium (#10981; StemCell) supplemented with ImmunoCult Human T Cell Activators (#10970; StemCell) and interleukin-2.

#### HTS on complementary DNA

Transcriptomic analysis was performed as previously described (33, 46). Briefly, RNA was extracted from PBMCs or T-blasts (NucleoMag RNA kit for magnetic bead-based RNA purification, #744350; Macherey-Nagel). DNA was eliminated with DNaseI (#M03035; Ozyme). RNA was reverse-transcribed to generate cDNA (PrimeScript RT reagent kit with gDNA Eraser [Perfect Real Time], #RR047Q; Takara), the second strand was synthesized (Second-Strand cDNA Synthesis Kit, #A48570; Thermo Fisher Scientific), and the resulting cDNA was purified (AMPure XP Reagent, #A63881; Beckman Coulter). We then sequenced 10–25 ng purified double-stranded cDNA, using the previously described Agilent panel of IEI genes for capture. Data were then aligned as previously described (33, 46). Sashimi plots were drawn with IGV, using splice junctions representing at least 5% of the mean coverage of the respective gene as the cutoff for minimal coverage.

#### Flow cytometry protein expression

Intracellular flow cytometry was performed as follows. For BTK, whole-blood cells were first subjected to extracellular staining with anti-CD14-Pacific blue (clone M5E2, #558121; BD) and anti-CD19 FITC (clone J3-119, #A07768; Beckman) antibodies, permeabilized with PhosphoFlow Lyse/fix buffer (#558049; Becton Dickinson) and Phosphoflow Perm/Wash Buffer I (#557885; Becton Dickinson), and then incubated with monoclonal anti-BTK AF647 antibody (clone 53/BTK, #558528; Becton Dickinson) or the corresponding AF647 isotype (clone MOPC-173, #558053; Becton Dickinson). For SAP, T-blasts were first permeabilized with a 0.5% BSA 0.5% saponin buffer. They were then incubated with or without murine monoclonal antibody (clone 1C9, #H00004068-M01; Abnova), with an AlexaFluor488 goat anti-mouse secondary antibody for detection (Thermo Fisher Scientific). For WASp, T-blasts were permeabilized with Cytofix/Cytoperm (#554714; Becton Dickinson) and incubated with monoclonal anti-WASp PE antibody (clone 5E5, custom reference; Becton Dickinson) or the corresponding PE isotype (normal mouse IgG1, Becton Dickinson). DOCK8 staining was performed as previously described (31). Briefly, whole-blood cells were permeabilized with Cytofix/Cytoperm (#554714; Becton

Dickinson) and incubated with clone EPR12511 (#ab175208; Abcam) or left unstained. A goat AF647-coupled secondary antibody against rabbit IgG (polyclonal, #ab150083; Abcam) was used for detection.

#### Degranulation or cytotoxicity assay

Degranulation assays were performed with Vγ9<sup>+</sup>Vδ2<sup>+</sup> T cells as previously described (47). Cytotoxic activity was assessed as previously described (48). Briefly for the cytotoxic activity assay, PBMCs from patients, parents, or normal controls were cultured with phytohemagglutinin (1/700 dilution; Difco) and IL-2 (20 IU/ml; Valbiotech) for 24 h. We then added IL-2 (40 IU/ml) and incubated the cells for 6 days. The lysis of Fas-deficient L1210-3 target cells (10<sup>4</sup> chromium<sup>51</sup>-loaded L1210 cells) was assessed in a standard 4-h release assay in the presence of monoclonal anti-CD3 antibody (OKT3; Orthoclone). The effector/target ratio was calculated from the number of CD8<sup>+</sup> T cells, as determined by flow cytometry.

#### Online supplemental material

Fig. S1 shows the evidence for DOCK8 revertant at genomic level in P4. Fig. S2 shows the additional Sashimi plots for DOCK8 (P4) and NFKB1 (P7). Fig. S3 shows the view for STXBP2 in silico prediction by SpliceAI and Pangolin. Table S1 shows a summary of the phenotype of the patients and their relatives. Table S2 shows the effects of the seven intronic variants predicted by SpliceAI and Pangolin. Table S3 shows the alignment and calling of the various variants in a 30X downsampling experiment.

#### Data availability

All data are either included in the manuscript or available upon request.

### Ethics statement

#### Consent to participate

Written informed consent to participate was obtained from the patients or their parents.

#### Consent for publication

Consent to publish this report was obtained from the patients or their parents. All the authors approved the final version of the manuscript.

#### Ethics approval

Informed consent for participation in this study was obtained in accordance with local regulations, with approval from the Institutional Review Board.

### Acknowledgments

The Laboratory of Human Genetics of Infectious Diseases is supported by the Howard Hughes Medical Institute, The Rockefeller University, the St. Giles Foundation, the French National Research Agency (ANR) under the “Investments for the Future” program (ANR-10-IAHU-01), the Integrative Biology of Emerging Infectious Diseases Laboratory of Excellence (ANR-10-

LABX-62-IBEID), the Square Foundation, Grandir - Fonds de solidarité pour l’enfance, William E. Ford, General Atlantic’s Chairman and Chief Executive Officer, Gabriel Caillaux, General Atlantic’s Co-President, Managing Director and Head of Business in EMEA, and the General Atlantic Foundation, Institut National de la Santé et de la Recherche Médicale, and the University of Paris Cité. P. Bastard was supported by the French Foundation for Medical Research (EA20170638020), the MD-PhD program of the Imagine Institute (with the support of the Fondation Bettencourt-Schueler), and a “Poste CCA-INSERM-Bettencourt” (with the support of the Fondation Bettencourt-Schueler).

Author contributions: N. Alioua: conceptualization, formal analysis, investigation, validation, visualization, and writing—original draft, review, and editing. N. Lambert: investigation. M. Puel: conceptualization, investigation, and methodology. S. Hanein: formal analysis. P. Bastard: investigation, resources, and writing—review and editing. M. Fusaro: resources and writing—review and editing. M. Jaffray: resources. B. Medel: formal analysis, investigation, resources, and visualization. L. Khellaf: data curation. Y. Seeleuthner: resources and software. M. Perin: data curation and formal analysis. C. Jacques: investigation. M. Pasquet: resources. L. Olivier: writing—review and editing. F. Sepulveda: methodology and supervision. T. Le Voyer: writing—review and editing. A. Cobat: resources. P. Nitschke: data curation and software. L. Galicier: resources and writing—review and editing. N. Schleinitz: investigation, resources, and writing—review and editing. E. Oksenhendler: resources. M. Malphettes: resources. B. Neven: resources. D. Moshous: resources and writing—review and editing. F. Suarez: resources. C. Fieschi: resources and writing—review and editing. J.-L. Casanova: funding acquisition, project administration, resources, supervision, and writing—review and editing. G. de Saint Basile: data curation, methodology, validation, and writing—review and editing. G. Dorval: formal analysis, methodology, software, and validation. C. Picard: project administration, resources, and writing—review and editing. J. Bustamante: resources and writing—review and editing. P. Zhang: data curation, formal analysis, investigation, methodology, software, validation, and writing—review and editing. J. Rosain: conceptualization, formal analysis, investigation, project administration, supervision, validation, and writing—original draft, review, and editing.

Disclosures: L. Galicier reported personal fees from Recordati, Amgen, and Novartis outside the submitted work. No other disclosures were reported.

Submitted: 22 March 2025

Revised: 7 May 2025

Accepted: 25 June 2025

### References

1. Meyts, I., B. Bosch, A. Bolze, B. Boisson, Y. Itan, A. Belkadi, V. Pedergana, L. Moens, C. Picard, A. Cobat, et al. 2016. Exome and genome sequencing for inborn errors of immunity. *J. Allergy Clin. Immunol.* 138: 957–969. <https://doi.org/10.1016/j.jaci.2016.08.003>
2. King, J.R., L.D. Notarangelo, and L. Hammarström. 2021. An appraisal of the Wilson & Jungner criteria in the context of genomic-based newborn

screening for inborn errors of immunity. *J. Allergy Clin. Immunol.* 147: 428–438. <https://doi.org/10.1016/j.jaci.2020.12.633>

3. Engelbrecht, C., M. Urban, M. Schoeman, B. Paarwater, A. van Coller, D.R. Abraham, H. Cornelissen, R. Glashoff, M. Esser, M. Möller, et al. 2021. Clinical utility of whole exome sequencing and targeted panels for the identification of inborn errors of immunity in a resource-constrained setting. *Front. Immunol.* 12:665621. <https://doi.org/10.3389/fimmu.2021.665621>

4. Similuk, M.N., J. Yan, R. Ghosh, A.J. Oler, L.M. Franco, M.R. Setzer, M. Kamen, C. Jodarski, T. DiMaggio, J. Davis, et al. 2022. Clinical exome sequencing of 1000 families with complex immune phenotypes: Toward comprehensive genomic evaluations. *J. Allergy Clin. Immunol.* 150: 947–954. <https://doi.org/10.1016/j.jaci.2022.06.009>

5. Hurabielle, C., T.N. LaFlam, M. Gearing, and C.J. Ye. 2024. Functional genomics in inborn errors of immunity. *Immunol. Rev.* 322:53–70. <https://doi.org/10.1111/imr.13309>

6. Celmeli, F., A. Oz, H.S. Kihtir, E.A. Ongun, A. Tekmenuray-Unal, S. Ceylaner, A. Aykut, S. Aydin, and S. Baris. 2024. Inborn errors of immunity in pediatric intensive care: Prevalence, characteristics, and prognosis. *J. Clin. Immunol.* 45:25. <https://doi.org/10.1007/s10875-024-01823-5>

7. Brakta, C., A.-C. Tabet, M. Puel, M. Pacault, M.-C. Stolzenberg, C. Goudet, M. Merger, H. Reumaux, N. Lambert, N. Alioua, et al. 2024. 2q33 deletions underlying syndromic and non-syndromic CTLA4 deficiency. *J. Clin. Immunol.* 45:46. <https://doi.org/10.1007/s10875-024-01831-5>

8. Singh, N., P. Ranganath, A. Jayaram, P. Jhawar, U. Kotecha, J. Jannardhanan, H. Kumar, K.A. Sudheer, S.M.N. Ali, K. Arigela, et al. 2024. Clinical and molecular profile of 20 patients with DOCK8 deficiency—a single-center experience from Southern India. *Immunol. Res.* 73:8. <https://doi.org/10.1007/s12026-024-09571-9>

9. Wright, C.F., D.R. FitzPatrick, and H.V. Firth. 2018 May. Paediatric genomics: Diagnosing rare disease in children. *Nat. Rev. Genet.* 19:253–268. <https://doi.org/10.1038/nrg.2017.116>

10. Fusaro, M., J. Rosain, V. Grandin, N. Lambert, S. Hanein, C. Fourrige, N. Renaud, M. Gil, S. Chevalier, W.A. Chahla, et al. 2021. Improving the diagnostic efficiency of primary immunodeficiencies with targeted next-generation sequencing. *J. Allergy Clin. Immunol.* 147:734–737. <https://doi.org/10.1016/j.jaci.2020.05.046>

11. PFMG2025 contributors. 2025. PFMG2025—integrating genomic medicine into the national healthcare system in France. *Lancet Reg. Health Eur.* 50:101183. <https://doi.org/10.1016/j.lanepe.2024.101183>

12. Casanova, J.L. 2025. Human immunity. *J. Hum. Immun.* 1:e20250001. <https://doi.org/10.70962/jhi.20250001>

13. Poli, M.C., I. Aksentijevich, A.A. Bousfiha, C. Cunningham-Rundles, S. Hambleton, C. Klein, T. Morio, C. Picard, A. Puel, N. Rezaei, et al. 2025. Human inborn errors of immunity: 2024 update on the classification from the international union of immunological societies expert committee. *J. Hum. Immun.* 1:e20250003. <https://doi.org/10.70962/jhi.20250003>

14. Walker, L.C., M.d.l. Hoya, G.A.R. Wiggins, A. Lindy, L.M. Vincent, M.T. Parsons, D.M. Canson, D. Bis-Brewer, A. Cass, A. Tchourbanov, et al. 2023. Using the ACMG/AMP framework to capture evidence related to predicted and observed impact on splicing: Recommendations from the ClinGen SVI Splicing Subgroup. *Am. J. Hum. Genet.* 110:1046–1067. <https://doi.org/10.1016/j.ajhg.2023.06.002>

15. Ellingford, J.M., J.W. Ahn, R.D. Bagnall, D. Baralle, S. Barton, C. Campbell, K. Downes, S. Ellard, C. Duff-Fraser, D.R. FitzPatrick, et al. 2022. Recommendations for clinical interpretation of variants found in non-coding regions of the genome. *Genome Med.* 14:73. <https://doi.org/10.1186/s13073-022-01073-3>

16. Kuksa, P.P., E. Greenfest-Allen, J. Cifello, M. Ionita, H. Wang, H. Nicarretta, P.-L. Cheng, W.-P. Lee, L.-S. Wang, and Y.Y. Leung. 2022. Scalable approaches for functional analyses of whole-genome sequencing non-coding variants. *Hum. Mol. Genet.* 31:R62–R72. <https://doi.org/10.1093/hmg/ddac191>

17. Zhang, P., Q. Philippot, W. Ren, W.-T. Lei, J. Li, P.D. Stenson, P.S. Palacín, R. Colobran, B. Boisson, S.-Y. Zhang, et al. 2022. Genome-wide detection of human variants that disrupt intronic branchpoints. *Proc. Natl. Acad. Sci. USA.* 119:e221194119. <https://doi.org/10.1073/pnas.221194119>

18. Zhang, P., M. Chaldebas, M. Ogishi, F. Al Qureshah, K. Ponsin, Y. Feng, D. Rinchai, B. Milisavljevic, J.E. Han, M. Moncada-Vélez, et al. 2023. Genome-wide detection of human intronic AG-gain variants located between splicing branchpoints and canonical splice acceptor sites. *Proc. Natl. Acad. Sci. USA.* 120:e2314225120. <https://doi.org/10.1073/pnas.2314225120>

19. Jagannathan, K., S. Kyriazopoulou Panagiotopoulou, J.F. McRae, S.F. Darbandi, D. Knowles, Y.I. Li, J.A. Kosmicki, J. Arbelaez, W. Cui, G.B. Schwartz, et al. 2019 Jan 24. Predicting splicing from primary sequence with deep learning. *Cell.* 176:535–548.e24. <https://doi.org/10.1016/j.cell.2018.12.015>

20. Zeng, T., and Y.I. Li. 2022. Predicting RNA splicing from DNA sequence using Pangolin. *Genome Biol.* 23:103. <https://doi.org/10.1186/s13059-022-02664-4>

21. Richards, S., N. Aziz, S. Bale, D. Bick, S. Das, J. Gastier-Foster, W.W. Grody, M. Hegde, E. Lyon, E. Spector, et al. 2015. Standards and guidelines for the interpretation of sequence variants: A joint consensus recommendation of the American College of medical genetics and genomics and the association for molecular pathology. *Genet. Med.* 17:405–424. <https://doi.org/10.1038/gim.2015.30>

22. Tangye, S.G., W. Al-Herz, A. Bousfiha, C. Cunningham-Rundles, J.L. Franco, S.M. Holland, C. Klein, T. Morio, E. Oksenhendler, C. Picard, et al. 2022. Human inborn errors of immunity: 2022 update on the classification from the international union of immunological societies expert committee. *J. Clin. Immunol.* 42:1473–1507. <https://doi.org/10.1007/s10875-022-01289-3>

23. Schubach, M., T. Maass, L. Nazaretyan, S. Röner, and M. Kircher. 2024. CADD v1.7: Using protein language models, regulatory CNNs and other nucleotide-level scores to improve genome-wide variant predictions. *Nucleic Acids Res.* 52:D1143–D1154. <https://doi.org/10.1093/nar/gkad989>

24. Siepel, A., G. Bejerano, J.S. Pedersen, A.S. Hinrichs, M. Hou, K. Rosenbloom, H. Clawson, J. Spieth, L.W. Hillier, S. Richards, et al. 2005. Evolutionarily conserved elements in vertebrate, insect, worm, and yeast genomes. *Genome Res.* 15:1034–1050. <https://doi.org/10.1101/gr.3715005>

25. Pollard, K.S., M.J. Hubisz, K.R. Rosenbloom, and A. Siepel. 2010. Detection of nonneutral substitution rates on mammalian phylogenies. *Genome Res.* 20:110–121. <https://doi.org/10.1101/gr.097857.109>

26. Karczewski, K.J., L.C. Francioli, G. Tiao, B.B. Cummings, J. Alföldi, Q. Wang, R.L. Collins, K.M. Laricchia, A. Ganna, D.P. Birnbaum, et al. 2020. The mutational constraint spectrum quantified from variation in 141,456 humans. *Nature.* 581:434–443. <https://doi.org/10.1038/s41586-020-2308-7>

27. Taliun, D., D.N. Harris, M.D. Kessler, J. Carlson, Z.A. Szpiech, R. Torres, S.A.G. Taliun, A. Corvelo, S.M. Gogarten, H.M. Kang, et al. 2021. Sequencing of 53,831 diverse genomes from the NHLBI TOPMed Program. *Nature.* 590:290–299. <https://doi.org/10.1038/s41586-021-03205-y>

28. Halldorsson, B.V., H.P. Eggertsson, K.H.S. Moore, H. Hauswedell, O. Eiriksson, M.O. Ulfarsson, G. Palsson, M.T. Hardarson, A. Oddsson, B.O. Jansson, et al. 2022. The sequences of 150,119 genomes in the UK Biobank. *Nature.* 607:732–740. <https://doi.org/10.1038/s41586-022-04965-x>

29. All of Us Research Program Genomics Investigators. 2024. Genomic data in the all of us research program. *Nature.* 627:340–346. <https://doi.org/10.1038/s41586-023-06957-x>

30. Stenson, P.D., M. Mort, E.V. Ball, M. Chapman, K. Evans, L. Azevedo, M. Hayden, S. Heywood, D.S. Millar, A.D. Phillips, and D.N. Cooper. 2020. The human gene mutation database (HGMD®): Optimizing its use in a clinical diagnostic or research setting. *Hum. Genet.* 139:1197–1207. <https://doi.org/10.1007/s00439-020-02199-3>

31. Pillay, B.A., M. Fusaro, P.E. Gray, A.L. Statham, L. Burnett, L. Bezrodnik, A. Kane, W. Tong, C. Abdo, S. Winter, et al. 2021. Somatic reversion of pathogenic DOCK8 variants alters lymphocyte differentiation and function to effectively cure DOCK8 deficiency. *J. Clin. Invest.* 131:e142434. <https://doi.org/10.1172/JCI142434>

32. Villani, R.M., M.E. McKenzie, A.L. Davidson, and A.B. Spurdle. 2024. Regional-specific calibration enables application of computational evidence for clinical classification of 5' cis-regulatory variants in Mendelian disease. *Am. J. Hum. Genet.* 111:1301–1315. <https://doi.org/10.1016/j.ajhg.2024.05.002>

33. Boisson, M., C. Arrondel, N. Cagnard, V. Morinière, Z.A. Arkoub, H. Saei, L. Heidet, J. Kachmar, A. Hummel, B. Knebelmann, et al. 2023. A wave of deep intronic mutations in X-linked Alport syndrome. *Kidney Int.* 104: 367–377. <https://doi.org/10.1016/j.kint.2023.05.006>

34. Meuwissen, M.E.C., R. Schot, S. Buta, G. Oudesluys, S. Tinschert, S.D. Speer, Z. Li, L. van Unen, D. Heijmans, T. Goldmann, et al. 2016. Human USP18 deficiency underlies type 1 interferonopathy leading to severe pseudo-TORCH syndrome. *J. Exp. Med.* 213:1163–1174. <https://doi.org/10.1084/jem.20151529>

35. Boisson, B., Y. Honda, M. Ajiro, J. Bustamante, M. Bendavid, A.R. Gennery, Y. Kawasaki, J. Ichishima, M. Osawa, H. Nihira, et al. 2019. Rescue of recurrent deep intronic mutation underlying cell type-dependent quantitative NEMO deficiency. *J. Clin. Invest.* 129:583–597. <https://doi.org/10.1172/JCI124011>

36. Roos, D., K. van Leeuwen, A.P. Hsu, D.L. Priel, A. Begtrup, R. Brandon, A. Rawat, P. Vignesh, M. Madkaikar, M.J. Stasia, et al. 2021. Hematologically important mutations: The autosomal forms of chronic granulomatous disease (third update). *Blood Cells. Mol. Dis.* 92:102596. <https://doi.org/10.1016/j.bcmd.2021.102596>

37. Stewart, O., C. Gruber, H.E. Randolph, R. Patel, M. Ramba, E. Calzoni, L.H. Huang, J. Levy, S. Buta, A. Lee, et al. 2025. Monoallelic expression can govern penetrance of inborn errors of immunity. *Nature*. 637: 1186–1197. <https://doi.org/10.1038/s41586-024-08346-4>

38. Tahiat, A., R. Belbouab, A. Yagoubi, S. Hakem, F. Fernini, M. Keddari, H. Belhadj, S. Touri, S. Aggoune, J. Stoddard, et al. 2024. Flow cytometry-based diagnostic approach for inborn errors of immunity: Experience from Algeria. *Front. Immunol.* 15:1402038. <https://doi.org/10.3389/fimmu.2024.1402038>

39. Kanegae, H., A. Hoshino, T. Okano, T. Yasumi, T. Wada, H. Takada, S. Okada, M. Yamashita, T.-W. Yeh, R. Nishikomori, et al. 2018. Flow cytometry-based diagnosis of primary immunodeficiency diseases. *Allergol. Int.* 67:43–54. <https://doi.org/10.1016/j.alit.2017.06.003>

40. Frésard, L., C. Smail, N.M. Ferraro, N.A. Teran, X. Li, K.S. Smith, D. Bonner, K.D. Kernohan, S. Marwaha, Z. Zappala, et al. 2019. Identification of rare-disease genes using blood transcriptome sequencing and large control cohorts. *Nat. Med.* 25:911–919. <https://doi.org/10.1038/s41591-019-0457-8>

41. Li, H., B. Handsaker, A. Wysoker, T. Fennell, J. Ruan, N. Homer, G. Marth, G. Abecasis, R. Durbin, and 1000 Genome Project Data Processing Subgroup. 2009. The sequence alignment/map format and SAMtools. *Bioinformatics*. 25:2078–2079. <https://doi.org/10.1093/bioinformatics/btp352>

42. Sherry, S.T., M.H. Ward, M. Kholodov, J. Baker, L. Phan, E.M. Smigielski, and K. Sirotnik. 2001. dbSNP: the NCBI database of genetic variation. *Nucleic Acids Res.* 29:308–311. <https://doi.org/10.1093/nar/29.1.308>

43. 1000 Genomes Project Consortium, A. Auton, L.D. Brooks, R.M. Durbin, E.P. Garrison, H.M. Kang, J.O. Korbel, J.L. Marchini, S. McCarthy, et al. 2015. A global reference for human genetic variation. *Nature*. 526:68–74. <https://doi.org/10.1038/nature15393>

44. Karczewski, K.J., L.C. Francioli, G. Tiao, B.B. Cummings, J. Alfoldi, Q. Wang, R.L. Collins, K.M. Laricchia, A. Ganna, D.P. Birnbaum, et al. 2019. Variation across 141,456 human exomes and genomes reveals the spectrum of loss-of-function intolerance across human protein-coding genes. *bioRxiv*. <https://doi.org/10.1101/531210> (Preprint posted August 13, 2019).

45. Goossens, D., L.N. Moens, E. Nelis, A.-S. Lenaerts, W. Glassee, A. Kalbe, B. Frey, G. Kopal, P. De Jonghe, P. De Rijk, and J. Del-Favero. 2009. Simultaneous mutation and copy number variation (CNV) detection by multiplex PCR-based GS-FLX sequencing. *Hum. Mutat.* 30:472–476. <https://doi.org/10.1002/humu.20873>

46. Dorval, G., G. Le Gac, V. Morinière, C. Ka, C. Goursaud, B. Knebelmann, P. Marijon, S. Nambot, N. Cagnard, P. Nitschlké, et al. 2024. Targeted RNAseq from patients' urinary cells to validate pathogenic noncoding variants in autosomal dominant polycystic kidney disease genes: A proof of concept. *Kidney Int.* 106:532–535. <https://doi.org/10.1016/j.kint.2024.05.029>

47. Jorisch-Mühlebach, O., D. Pitts, R. Tinner, H.Y. Teh, C. Roelli, S. Prader, S. Vavassori, and J. Pachlopnik Schmid. 2024. A degranulation assay using Vγ9Vδ2 T cells for the rapid diagnosis of familial hemophagocytic syndromes. *Front Immunol.* 15:1391967. <https://doi.org/10.3389/fimmu.2024.1391967>

48. Stepp, S.E., R. Dufourcq-Lagelouse, F. Le Deist, S. Bhawan, S. Certain, P.A. Mathew, J.I. Henter, M. Bennett, A. Fischer, G. de Saint Basile, and V. Kumar. 1999. Perforin gene defects in familial hemophagocytic lymphohistiocytosis. *Science*. 286:1957–1959. <https://doi.org/10.1126/science.286.5446.1957>

## Supplemental material

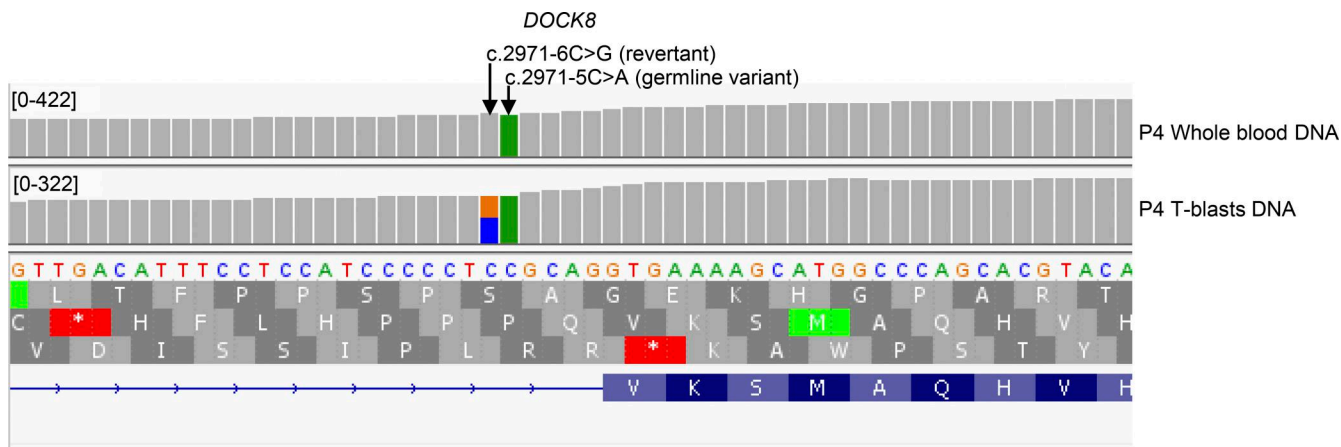


Figure S1. IGV view of HTS of P4's genomic DNA extracted from whole blood (top) or T-blasts (bottom), in *DOCK8* at the junction of intron 24 and exon 25.

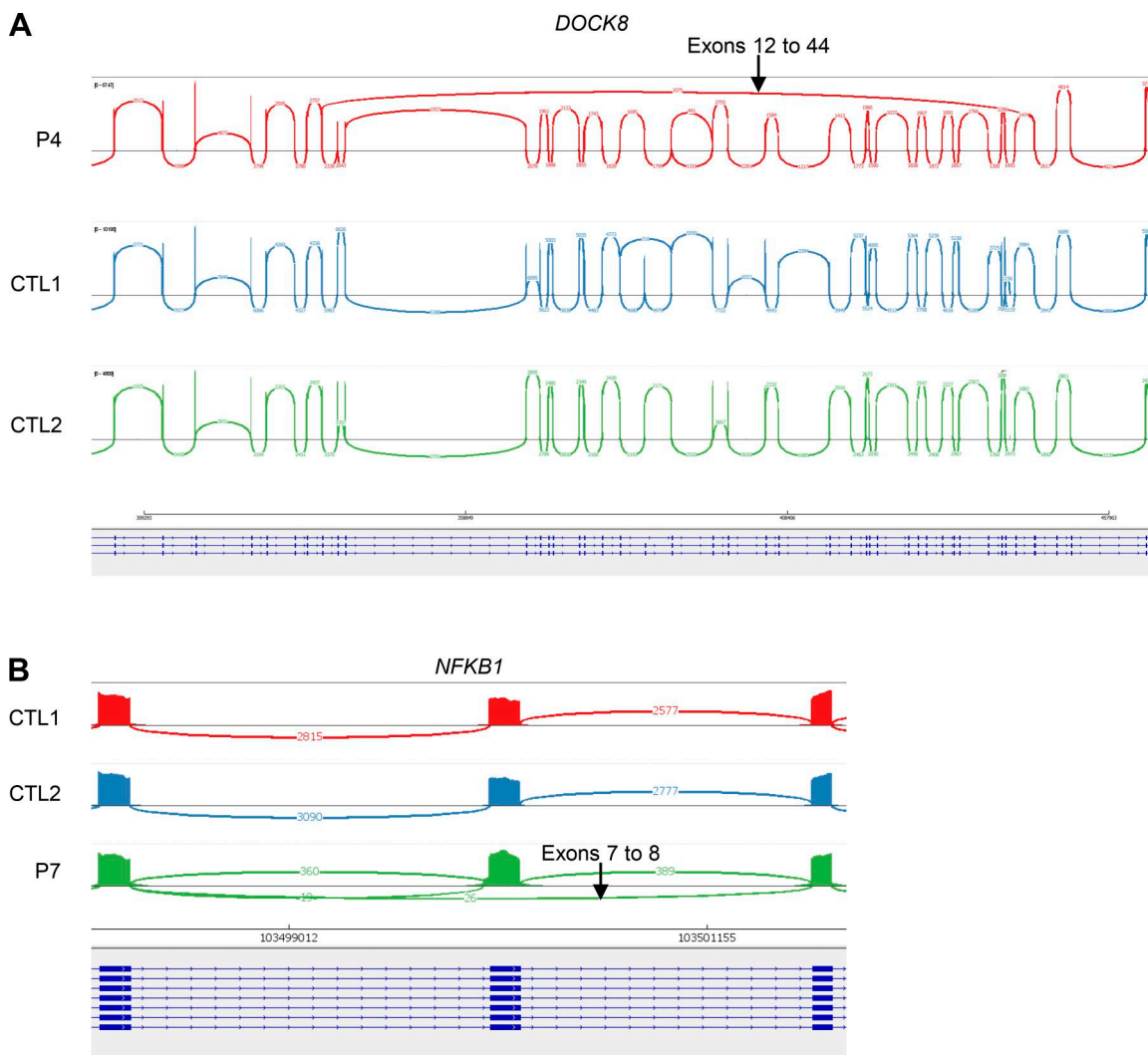


Figure S2. **Sashimi view of RNA sequencing in P3 and P7. (A and B)** Sashimi plots of (A) *DOCK8* with the skipping of exons 13–43 in T-blasts from P4 and (B) *NFKB1* exon 8 skipping in T-blasts from P7.

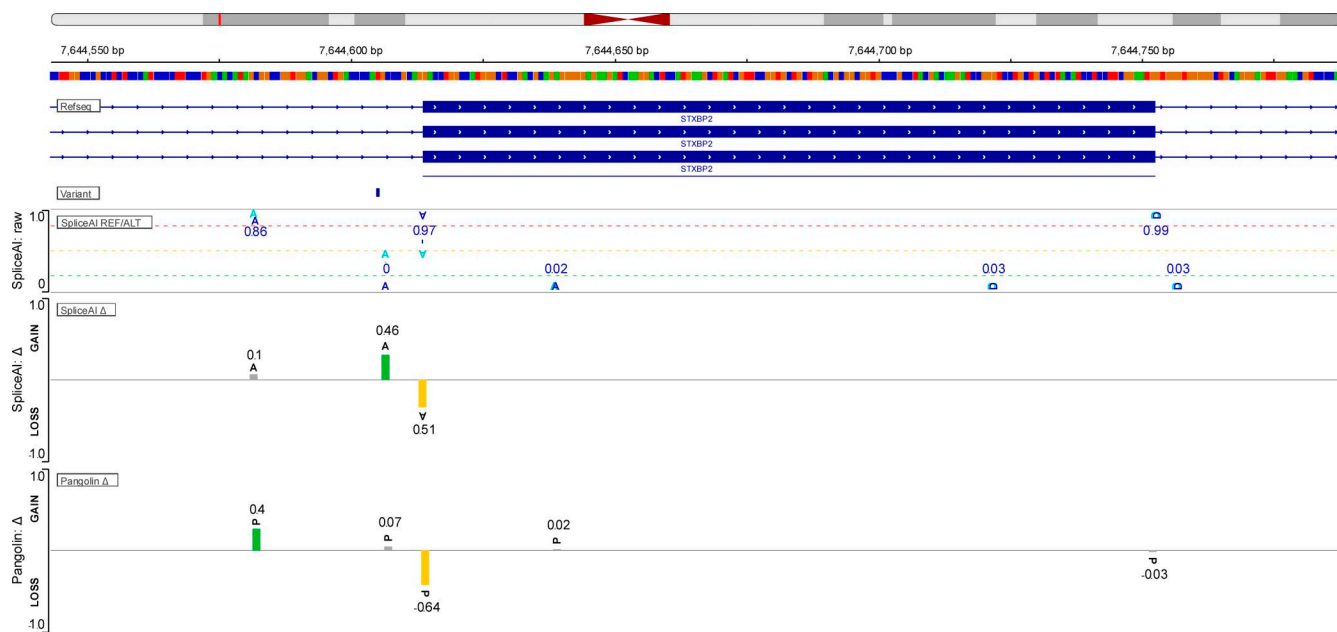


Figure S3. SpliceAI and Pangolin view from <https://spliceailookup.broadinstitute.org/> of AG-gain variant c.1108-9T>A in STXBP2.

Provided online are Table S1, Table S2, and Table S3. Table S1 shows the summary of clinical and basic immunological testing of index cases from the seven kindreds and their familial history. Table S2 shows the effects of the seven intronic variants predicted by SpliceAI and Pangolin. Table S3 shows the depth coverage of aligned and called intronic variants in the original and in 30X downsampling projects.